

Unsaturated Compounds of the Main Group Elements. Indenyllithium Tetramethylethylenediamine

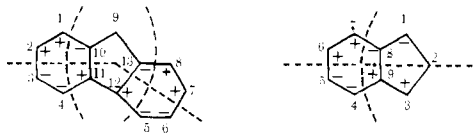
Wendell E. Rhine and G. D. Stucky*

Contribution from the Department of Chemistry and the Materials Research Laboratory,
University of Illinois, Urbana, Illinois 61801. Received July 1, 1974

Abstract: The molecular structure and charge distribution in indenyllithium tetramethylethylenediamine, $C_4H_7LiN_2C_6H_{16}$, have been studied by single-crystal X-ray diffraction, nuclear magnetic resonance, and semiempirical molecular orbital calculations. The title compound crystallizes in the space group $P\bar{1}$ of the triclinic system with two molecules in a cell of dimension, $a = 8.454$ (10) Å, $b = 16.445$ (19) Å, $c = 6.045$ (7) Å, $\cos \alpha = -0.3327$ (15), $\cos \beta = -0.3201$ (13), $\cos \gamma = 0.1598$ (14), and $\rho_{\text{calcd}} = 1.11$ g cm⁻³. Data (3285) were measured on a diffractometer and refined to a weighted R factor on $|F|$ of 0.055. The lithium atom is coordinated to one bidentate tetramethylethylenediamine molecule and to the indenyl group in an approximate h^3 configuration with three ring carbon lithium atom distances of 2.298 ± 0.019 Å and two ring carbon lithium atom distances of 2.377 ± 0.002 Å. The interaction of the N-Li-N group with the indenyl ring is discussed in terms of the results of INDO calculations. Nmr spectra measured in different solvents suggest that indenyllithium exists as a solvent separated species in dimethoxyethane. The charge distribution for the indenyl carbanion, as inferred from solution nmr data, is presented and compared with the INDO results.

There is now available a limited amount of data which suggests¹⁻³ that the 2s and 2p valence orbitals of the lithium atom interact with the highest occupied molecular orbital (HOMO) of a π carbanion in a stereochemically significant fashion. Thus, not only the position of the lithium atom with respect to the delocalized carbanion but also the orientation of the B-Li-B fragment (B = coordinated base atom, such as a tertiary amine nitrogen or ether oxygen atom) may be influenced by the carbanion HOMO as well as by the expected dipolar electrostatic interactions. The carbanions which have been examined are benzyl,¹ triphenylmethyl,² fluorenyl,³ and naphthalene.⁴ Additional data are obviously needed in order to investigate the relative importance of directed covalent bonding as opposed to electrostatic dipolar interactions.³

The geometrical relation of the fluorenyl and indenyl systems is obvious, *i.e.*, dibenzo- and benzocyclopentadiene, respectively. Both are relatively stable carbanions with indene having a lower pK_a value (19) than fluorene (23).^{5,6} An important difference is in the properties of the HOMO's of the two carbanions as illustrated below. Previous consid-



erations^{3,4} would suggest that a disolvated lithium atom would be located on a nodal surface of the HOMO of the indenyl carbanion in such a way that the LiB_2 plane is approximately parallel to the nodal surface permitting the available lithium atom p orbital to bridge across the p_z orbitals of 1,3 carbon atoms in an allylic fashion. The σ , as well as the dipolar, interaction would result in the lithium atom being most closely associated with the carbon atoms which are closest to the INDO calculated minimum of the electrostatic potential energy surface.

In the case of the fluorenyl carbanion, the 1,9 carbon atoms have the proper symmetry and the largest coefficients (of any allylic set) in the HOMO of the carbanion. In the indenyl anion, the 1,3 carbon atoms have the largest coefficients in the HOMO and are of the proper symmetry. These considerations would indicate that (1) the lithium atom would be positional above the five-membered ring with (2) the B_2Li plane nearly perpendicular to a vector joining C(1) and C(3) rather than outside the five-mem-

bered ring and associated with C(1) and C(7) as is observed for the C(1) and C(9) carbon atoms in fluorenyllithium bisquinuclidine.

The specific compound isolated and chosen for study was indenyllithium tetramethylethylenediamine. This paper describes the isolation and structural and nmr characterization of this material.

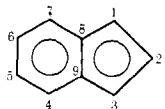
Experimental Section

Synthesis. Indenyllithium tetramethylethylenediamine, $C_9H_7Li(N_2C_6H_{16})$, was obtained by adding an 0.013 mol sample of freshly distilled indene to 200 ml of dry hexane and 1.5 g of *N,N,N',N'*-tetramethylethylenediamine (TMEDA) under a nitrogen atmosphere. A 10-ml (0.013 mol) sample of *n*-butyllithium in hexane was added to the flask *via* syringe. A precipitate formed immediately, but dissolved when the solution was heated to reflux. After cooling the reaction solution, a mass of yellow crystals formed. The reaction mixture was transferred to a drybox where the crystals were isolated by filtration. Suitable crystals for X-ray analysis were obtained by recrystallizing the indenyllithium TMEDA from benzene. Recrystallization gave almost colorless crystals.

Solution Data. Samples for nmr spectra were prepared in an argon filled drybox at concentrations of about 15% by weight. The spectra were obtained on a Varian A60 spectrometer. Chemical shifts are reported relative to an internal standard, TMS.

Crystallographic Data. Precession photographs showed that the crystals are triclinic ($P\bar{1}$ or $P1$). Successful refinement of the structure later confirmed the centric space group, $P\bar{1}$. The lattice parameters ($T = 23^\circ$, λ 0.71069 Å) determined from the least-squares refinement of 12 centered reflections measured as previously described^{3,4} are $a = 8.454$ (10) Å, $b = 16.445$ (19) Å, $c = 6.045$ (7) Å, $\cos \alpha = -0.3327$ (15), $\cos \beta = -0.3201$ (13), and $\cos \gamma = 0.1598$ (14)°. The calculated density for two molecules per unit cell is 1.11 g/cm³. The experimental density was not measured because of reactivity with suitable solvents.

The crystal, an elongated parallelepiped of dimension $0.5 \times 0.3 \times 0.3$ mm, was oriented for data collection so that the c^* axis was coincident with the ϕ axis of the Picker diffractometer. Several ω scans gave a full peak width at half-height of 0.15° indicating the mosaicity was acceptably low for data collection. A survey of various peaks showed that a 2θ scan of 2.0° was sufficient to obtain all the peak intensity. A full form of data (hkl , $\bar{h}kl$, $h\bar{k}l$, and $\bar{h}\bar{k}l$) was measured to $2\theta_{\text{max}} = 54^\circ$, giving a total of 3285 unique reflections. Of the unique data, 1451 reflections were considered observed using the criteria, $I_{\text{obsd}} > 3\sigma_c(I)$ where $\sigma_c(I)$ is as defined previously.^{3,4} The F 's which were observed to have negative intensities were set equal to zero. All unique reflections were used in the structure refinement. The remainder of the data collection details are the same as reported previously.^{3,4}

Table I. Positional Parameters for the Nonhydrogen Atoms of $C_9H_7Li(N_2C_6H_{16})$


	x	y	z
C(1)	0.6310 (2)	0.2958 (1)	0.3027 (4)
C(2)	0.6362 (3)	0.3675 (1)	0.5043 (5)
C(3)	0.7044 (2)	0.3444 (1)	0.7147 (5)
C(4)	0.8261 (2)	0.1964 (2)	0.7785 (4)
C(5)	0.8563 (2)	0.1122 (2)	0.6588 (4)
C(6)	0.8105 (2)	0.0821 (1)	0.4065 (4)
C(7)	0.7350 (2)	0.1367 (1)	0.2725 (4)
C(8)	0.7023 (2)	0.2245 (1)	0.3860 (3)
C(9)	0.7492 (2)	0.2548 (1)	0.6474 (3)
AC(1)	0.2962 (3)	0.1089 (2)	0.2017 (4)
AC(2)	0.4064 (3)	0.1291 (1)	0.6187 (4)
AC(3)	0.1495 (3)	0.3882 (2)	0.3806 (5)
AC(4)	0.2774 (3)	0.4291 (1)	0.7971 (5)
AC(5)	0.1511 (7)	0.2095 (5)	0.4530 (8)
AC(6)	0.1572 (5)	0.2945 (3)	0.6330 (7)
N(1)	0.3191 (2)	0.1730 (1)	0.4397 (3)
N(2)	0.2433 (2)	0.3568 (1)	0.5822 (3)
Li	0.4546 (3)	0.2793 (2)	0.5060 (5)
AC(5)'	0.1887 (2)	0.2199 (2)	0.5837 (5)
AC(6)'	0.1077 (1)	0.2964 (1)	0.4729 (3)

Solution and Refinement of Structure. The structure of $C_9H_7Li(N_2C_6H_{16})$ was solved by the use of direct methods (symbolic addition procedure) with the symbolic program MULTAN.⁷ MULTAN gave 16 sets of phases with the same figure of merit. All E-maps examined showed possible positions for the indenyl anion. The correct solution was obtained by some unusual trial and error direct method procedures.

After six carbon atoms were placed correctly, the rest of the atoms were found in the subsequent Fourier. After one cycle of full-matrix least-squares using the program ORFLSD, the R factor was

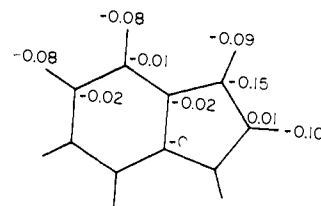
$$R_2 = (\sum w(F_o - F_c)^2 / \sum wF_o^2)^{1/2} = 0.22$$

Isotropic refinement on all nonhydrogen atoms gave convergence at $R_2 = 0.16$. The hydrogen atoms were then added at the calculated positions using the program HYGEM. Each hydrogen

Table II. Thermal Parameters for the Atoms of $C_9H_7Li(N_2C_6H_{16})$

	Anisotropic Thermal Parameters for Nonhydrogen Atoms					
	β_{11}	β_{22}	β_{33}	β_{12}	β_{13}	β_{23}
C(1)	0.0206 (4)	0.0061 (1)	0.0547 (11)	0.0004 (2)	0.0159 (5)	0.0090 (3)
C(2)	0.0219 (4)	0.0041 (1)	0.0295 (16)	-0.0004 (2)	0.0249 (7)	0.0073 (4)
C(3)	0.0191 (4)	0.0054 (1)	0.0549 (11)	-0.0034 (2)	0.0145 (5)	-0.0011 (3)
C(4)	0.0126 (3)	0.0085 (1)	0.0354 (9)	-0.0012 (2)	0.0046 (4)	0.0057 (3)
C(5)	0.0157 (3)	0.0071 (1)	0.0576 (11)	0.0011 (2)	0.0117 (5)	0.0105 (4)
C(6)	0.0175 (3)	0.0047 (1)	0.0593 (11)	-0.0003 (2)	0.0154 (4)	0.0034 (3)
C(7)	0.0151 (3)	0.0056 (1)	0.0369 (8)	-0.0009 (1)	0.0095 (4)	0.0025 (3)
C(8)	0.0125 (3)	0.0044 (1)	0.0357 (7)	-0.0011 (1)	0.0091 (3)	0.0030 (2)
C(9)	0.0118 (3)	0.0047 (1)	0.0370 (8)	-0.0020 (1)	0.0083 (4)	0.0009 (2)
AC(1)	0.0359 (6)	0.0096 (2)	0.0571 (11)	-0.0087 (2)	0.0121 (6)	0.0005 (3)
AC(2)	0.0237 (4)	0.0077 (1)	0.0649 (11)	-0.0034 (2)	0.0078 (6)	0.0092 (3)
AC(3)	0.0328 (6)	0.0119 (2)	0.0913 (17)	0.0060 (3)	0.0159 (8)	0.0109 (5)
AC(4)	0.0323 (6)	0.0074 (1)	0.0824 (14)	0.0007 (2)	0.0231 (7)	-0.0006 (4)
AC(5)	0.0140 (6)	0.0078 (3)	0.0696 (21)	-0.0027 (3)	0.0061 (9)	0.0051 (6)
AC(6)	0.0214 (7)	0.0076 (2)	0.0710 (20)	-0.0012 (3)	0.0245 (10)	0.0042 (6)
AC(5)'	0.0186 (35)	0.0037 (8)	0.1463 (170)	0.0028 (13)	0.0417 (67)	0.0147 (33)
AC(6)'	0.0130 (20)	0.0071 (9)	0.0740 (78)	0.0020 (10)	0.0188 (34)	0.0114 (23)
N(1)	0.0144 (3)	0.0050 (1)	0.0492 (7)	-0.0018 (1)	0.0085 (3)	0.0045 (2)
N(2)	0.0194 (3)	0.0050 (1)	0.0658 (9)	0.0001 (1)	0.0158 (4)	0.0031 (2)
Li	0.0156 (5)	0.0048 (1)	0.0489 (13)	-0.0013 (2)	0.0115 (6)	0.0042 (3)

Isotropic Thermal Parameters for Indenyl Hydrogen Atoms					
H(1)	5.2 (4)	H(3)	5.7 (4)	H(5)	5.7 (5)
H(2)	5.8 (4)	H(4)	6.9 (5)	H(6)	6.5 (5)
				H(7)	4.8 (4)

**Figure 1.** Gross INDO atomic charges for the indenyl group.

atom was given an isotropic thermal parameter equal to that of its parent carbon atom and placed 1.0 Å from that atom. One more cycle of isotropic refinement of nonhydrogen atoms gave $R_2 = 0.128$. Further refinement after conversion to anisotropic thermal parameters led to R factors

$$R_1 = \Sigma F_o - F_c / \Sigma F_o = 0.066 \text{ (observed data)}$$

$$R_2 = 0.066 \text{ (all data)}$$

A difference Fourier showed peaks of $0.5 \text{ e}/\text{\AA}^3$ in the vicinity of the tetramethylethylenediamine ethylenic carbons, indicating possible disorder in the TMEDA moiety. Two methylene carbon atoms were added to the refinement at the positions indicated by the difference Fourier. The four methylene carbon atoms were given equal isotropic temperature factors, and the multiplicity was refined. This indicated that the peaks from the difference Fourier represented $1/5$ of a carbon atom. The refinement was continued using multiplicities of 0.80 and 0.20 for the methylene carbon atoms and led to final values of R_1 and R_2 (after varying the indenyl hydrogen atom positions and isotropic thermal parameters to convergence): $R_1 = 0.057$ (observed data), $R_2 = 0.055$ (all data).

$$\text{ERF} = [\Sigma w(F_o - F_c)^2 / (NO - NV)]^{1/2} = 1.34$$

where NO = number of observations and NV = number of variables. Statistical weights were used as defined previously^{3,4} with $K = 0.03$. A test of the weighting scheme showed no significant variation of $w(F_o - F_c)^2$ with the magnitude of the F_{OBS} or with respect to $\sin \theta/\lambda$.

The final positional and thermal parameters for the nonhydrogen atoms are contained in Tables I and II. Table III gives the indenyl hydrogen atom positions.⁸ Bond distances and angles are given in Tables IV and V. The average indenyl C-H distance was 0.96 Å.

Table III. Indenyl Hydrogen Atom Positions for $C_9H_7Li(N_2C_6H_{16})$

	x	y	z
H(1)	0.589 (2)	0.295 (1)	0.132 (3)
H(2)	0.594 (2)	0.425 (1)	0.504 (3)
H(3)	0.723 (2)	0.381 (1)	0.879 (3)
H(4)	0.858 (2)	0.214 (1)	0.948 (4)
H(5)	0.907 (2)	0.075 (1)	0.757 (3)
H(6)	0.832 (2)	0.175 (1)	0.329 (3)
H(7)	0.698 (2)	0.114 (1)	0.091 (3)
AC(1)H(1)	0.235	0.137	0.060
AC(1)H(2)	0.415	0.081	0.174
AC(1)H(3)	0.226	0.058	0.182
AC(2)H(1)	0.424	0.174	0.800
AC(2)H(2)	0.334	0.080	0.609
AC(2)H(3)	0.523	0.102	0.601
AC(3)H(1)	0.124	0.332	0.216
AC(3)H(2)	0.037	0.419	0.399
AC(3)H(3)	0.221	0.428	0.350
AC(4)H(1)	0.347	0.407	0.954
AC(4)H(2)	0.354	0.473	0.789
AC(4)H(3)	0.169	0.464	0.838
AC(5)H(1)	0.102	0.170	0.530
AC(5)H(2)	0.070	0.208	0.287
AC(6)H(1)	0.024	0.320	0.602
AC(6)H(2)	0.204	0.294	0.803

Table IV. Interatomic Distances (Å) for the Nonhydrogen Atoms in $C_9H_7Li(N_2C_6H_{16})$

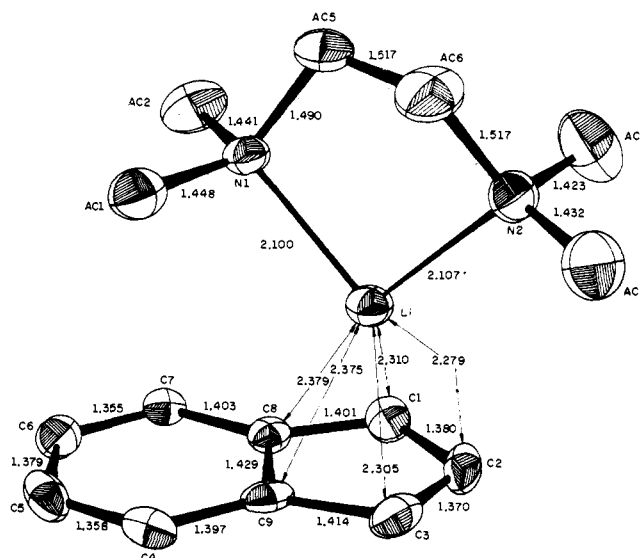
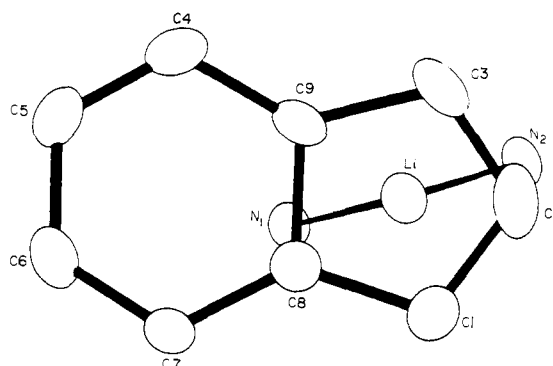
C(1)-H(1)	0.97 (2)	AC(1)-N(1)	1.448 (3)
C(2)-H(2)	0.96 (2)	AC(2)-N(1)	1.441 (3)
C(3)-H(3)	0.95 (2)	AC(3)-N(2)	1.432 (3)
C(4)-H(4)	0.92 (2)	AC(4)-N(2)	1.423 (3)
C(5)-H(5)	0.96 (2)	AC(5)-N(1)	1.467 (7)
C(6)-H(6)	1.02 (2)	AC(6)-N(2)	1.505 (5)
C(7)-H(7)	0.99 (2)	AC(5')-N(1)	1.57 (2)
C(1)-C(2)	1.380 (2)	AC(6')-N(2)	1.47 (2)
C(2)-C(3)	1.370 (2)	AC(5)-AC(6)	1.454 (8)
C(3)-C(9)	1.414 (3)	AC(5')-AC(6')	1.58 (3)
C(4)-C(9)	1.397 (2)	Li-C(1)	2.310 (4)
C(4)-C(5)	1.358 (2)	Li-C(2)	2.279 (4)
C(5)-C(6)	1.379 (3)	Li-C(3)	2.305 (4)
C(6)-C(7)	1.355 (2)	Li-C(8)	2.379 (4)
C(7)-C(8)	1.403 (3)	Li-C(9)	2.375 (4)
C(8)-C(9)	1.429 (3)	Li-N(1)	2.099 (4)
C(1)-C(8)	1.401 (3)	Li-N(2)	2.107 (4)

Table V. Bond Angles (deg) for the Nonhydrogen Atoms in $C_9H_7Li(N_2C_6H_{16})$

C(8)-C(1)-C(2)	108.1 (2)	AC(3)-N(2)-AC(4)	107.8 (2)
C(1)-C(2)-C(3)	109.9 (2)	AC(4)-N(2)-AC(6)	106.8 (2)
C(2)-C(3)-C(9)	107.9 (2)	AC(4)-N(2)-AC(6')	131.9 (6)
C(3)-C(9)-C(8)	106.9 (2)	AC(3)-N(2)-AC(6)	115.6 (2)
C(1)-C(8)-C(9)	107.1 (2)	AC(3)-N(2)-AC(6')	81.0 (5)
C(7)-C(8)-C(9)	118.1 (2)	Li-N(2)-AC(3)	110.6 (2)
C(4)-C(9)-C(8)	118.9 (2)	Li-N(2)-AC(4)	115.4 (2)
C(8)-C(4)-C(5)	120.4 (2)	C(2)-Li-N(1)	164.2 (2)
C(4)-C(5)-C(6)	121.2 (2)	C(8)-Li-N(2)	164.0 (2)
C(5)-C(6)-C(7)	120.3 (2)	C(8)-Li-N(1)	107.4 (1)
C(6)-C(7)-C(8)	121.1 (2)	C(2)-Li-N(2)	107.6 (1)
N(1)-Li-N(2)	86.4 (1)	AC(1)-N(1)-AC(2)	106.7 (2)
C(1)-Li-C(2)	35.0 (1)	AC(2)-N(1)-AC(5)	114.7 (3)
C(1)-Li-C(3)	58.4 (1)	AC(2)-N(1)-AC(5')	92.6 (8)
C(1)-Li-C(8)	58.1 (1)	AC(1)-N(1)-AC(5)	106.0 (2)
C(1)-Li-C(9)	34.7 (1)	AC(1)-N(1)-AC(5')	130.3 (9)
C(2)-Li-C(8)	57.8 (1)	Li-N(1)-AC(1)	116.5 (2)
		Li-N(1)-AC(2)	107.9 (2)

Discussion

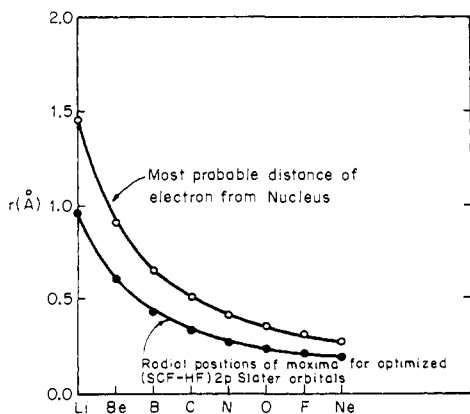
Molecular Structure of $C_9H_7Li(N_2C_6H_{16})$. The structure of indenyllithium TMEDA (Figure 2) consists of an indenyl moiety bound to a lithium atom which is also coordinated to an N,N,N',N' -tetramethylethylenediamine group. The coordination sphere of the lithium atom contains two ter-

**Figure 2.** Molecular structure of $C_9H_7Li(N_2C_6H_{16})$.**Figure 3.** Orientation of the N-Li-N group with respect to the indenyl plane in $C_9H_7Li(N_2C_6H_{16})$.

ary amine nitrogen atoms and one unsaturated organic anion as in the previous unsaturated organolithium structures.²⁻⁴ The lithium atom assumes a position over the five-member ring of the indenyl group, 2.279 (4) Å from C(2), 2.310 (4) Å from C(1), 2.305 (4) Å from C(3), 2.379 (4) Å from C(8), and 2.375 (4) Å from C(9). These values show that the lithium atom is not located over the center of the five-membered ring but is shifted toward C(2). The average Li-C distance to the five-membered ring carbon atoms is 2.33 Å, which is 0.10 Å less than the corresponding average Mg-C distances in bis(indenyl)magnesium.⁹ The differences in the ionic and atomic radii of Li^+ and Mg^{2+} is 0.05 Å, $Mg^{2+} > Li^+$ and $Mg > Li$. As in fluorenyllithium bisquinuclidine, the lithium atom is over a node in the HOMO of the carbanion. The N-Li-N plane makes an angle of approximately 18° with the nodal plane passing through C(2) (Figure 3). INDO calculations (Table VI) suggest that this orientation of the N-Li-N group with respect to the HOMO (A_2 symmetry) of the indenyl ring permits the efficient overlap of an empty lithium p orbital with the indenyl p_z orbitals, *i.e.*, the lithium atom is effective in bridging across a 1,3 carbon allylic system. More specifically, this is reflected in the relatively large magnitudes of the coefficients of the lithium p_y orbital (0.25) and the C(1) and C(3) p_z orbitals (0.50) as well as the $Li(p_y)$ -C(1)(p_z) and $Li(p_y)$ -C(3)(p_z) overlap integrals of 0.139 and -0.139, respectively. The latter can be compared with a C(5)(p_z)-C(6)(p_z) overlap integral of 0.25. The distance between the 1,3 carbon atoms in the indenyl ring is 2.252 (4) Å. This value compares well with the radial properties of the lithi-

Table VI. Highest Occupied Molecular Orbital Coefficients for the Isolated Indenyl Anion and for $[\text{Li}(\text{NH}_3)_2]$ Indenyl

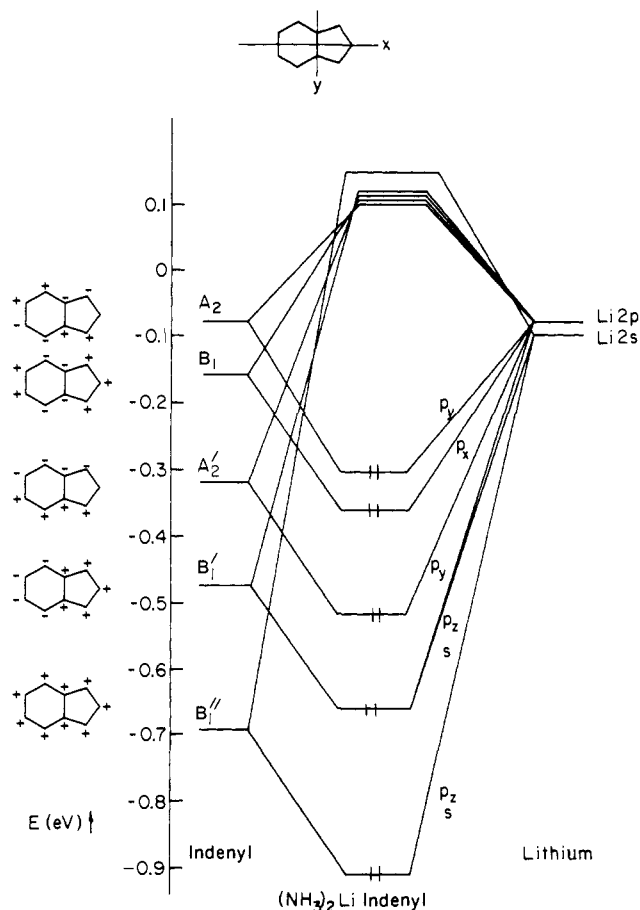
Atom	Isolated indenyl anion	$[\text{Li}(\text{NH}_3)_2]$ indenyl
C(1)	-0.56	-0.51
C(2)	0.00	0.0
C(3)	0.56	0.50
C(4)	-0.28	-0.35
C(5)	-0.25	-0.27
C(6)	0.25	0.25
C(7)	0.28	0.35
C(8)	-0.21	-0.12
C(9)	0.21	0.14
Li p_x		0.03
Li p_y		-0.25

**Figure 4.** Radial properties of the 2p atomic wave function for second row elements.

um atomic 2p wave function as shown in Figure 4.

There is another structural feature which has been observed in LiTMEDA delocalized π carbanions (naphthalene, anthracene, acenaphthylene, and indenyl) in which the lithium atom is located directly above an aromatic ring system. In indenyllithium TMEDA, the $\text{N}(1)\text{-Li-N}(2)$, $\text{C}(8)\text{-Li-N}(1)$, $\text{C}(2)\text{-Li-N}(2)$, and $\text{C}(2)\text{-Li-C}(8)$ angles add up to 359.2° ; *i.e.*, the lithium atom is nearly coplanar with four closely associated ligand atoms. In naphthalene (lithium TMEDA)₂, the $\text{N}(1)\text{-Li-N}(2)$, $\text{N}(1)\text{-Li-C}(2)$, $\text{N}(1)\text{-Li-C}(5)$, and $\text{C}(2)\text{-Li-C}(5)$ angles add up to 360.6° . In anthracene (Li TMEDA)₂, similar values of 359.8 and 361.4° are obtained for the angles involving the $\text{C}(11)\text{-C}(13)$ and $\text{C}(2)\text{-C}(12)$ carbon atom pairs, respectively. The consistency of the results are such that it seems reasonable that a specific intramolecular interaction is responsible.

The close approach of the lithium atom to carbon atoms 1, 2, and 3 is a general feature of metal-indenyl interactions^{15,16} and can be adequately explained by employing Pauling's resonating bond treatment¹⁷ or by a molecular orbital approach. Figure 5 shows the correlation between the lithium atomic orbitals and the indenyl π molecular orbitals. Similar correlations can be made with the indenyl σ MO's but they have been left out for simplicity. As illustrated, the INDO calculations show that the symmetry of the HOMO of the indenyl anion (A_2) is retained in the HOMO of the complex, a feature found in all lithium π carbanions that we have studied to date. Experimentally, this is reflected in the bond lengths of the carbanion (Figure 6); for example, the $\text{C}(7)\text{-C}(8)$ and $\text{C}(4)\text{-C}(9)$ bond lengths correspond to an antibonding contribution in the HOMO and average 1.400 (2) Å, while $\text{C}(6)\text{-C}(7)$ and $\text{C}(4)\text{-C}(5)$ correspond to a bonding interaction and average 1.357 (2) Å. The difference in these bond lengths (0.043 Å)

**Figure 5.** Correlation between lithium atomic and indenyl π molecular orbitals.

is very close to the difference predicted from Hückel π bond orders (0.040 Å),¹⁰ although the magnitudes of all the bond lengths, except $\text{C}(8)\text{-C}(9)$ are $0.01\text{-}0.03$ Å less than predicted by Hückel calculations. The five-membered ring (plane 5, Table VII) is slightly nonplanar with $\text{C}(1)$ and $\text{C}(3)$ being 0.014 (2) Å out of the plane of $\text{C}(2)$, $\text{C}(8)$, and $\text{C}(9)$ toward the lithium atom. There is some indication that $\text{H}(2)$ is on the same side of plane 5 as the lithium atom, while $\text{H}(1)$ and $\text{H}(3)$ are bent away from the lithium atom.

The average lithium-nitrogen bond length of 2.103 (4) is similar to the lithium-nitrogen atom bond lengths in $\text{Ph}_3\text{Me LiTMEDA}$. The N-Li-N angle of 86° agrees with the N-Li-N angles in ethylenediamine-type lithium compounds. The ethylenediamine group has some disorder associated with it, which is similar to that found in $\text{Ph}_3\text{Me LiTMEDA}$.³ It differs, however, in that there is not an equal population of the two possible forms and is best described by a model using multiplicities of 0.8 and 0.2 for the ethylenic carbon atoms in the TMEDA group. The anisotropic thermal parameters for the methyl group adequately compensated for any disorder in the methyl groups since the highest peak in the final difference Fourier map was 0.2 e/Å³.

Solution Nmr Data for Indenyllithium. The proton nmr spectra of indenyllithium TMEDA were recorded in benzene, diethyl ether, tetrahydrofuran (THF), and dimethoxyethane (DME) (Table VIII, Figure 7). Our results are compared to those previously reported for indenylsodium in THF.^{11,12} In DME, the proton nmr resonances are at higher field than observed for the sodium compound. It has been reported¹¹ that the size of the cation within the ion pair determines the proton shifts of the anion so that the smaller

Table VII

Plane	Atoms in Plane	Best Weighted Least-Square Planes				χ^2
		Equation of Plane				
1	C(1), C(2), C(3), C(4), C(5), C(6), C(7), C(8), C(9)	$-0.9719x - 0.2032y - 0.0122z + 6.2967 = 0$				253.7
2	C(4), C(5), C(6), C(7), C(8), C(9)	$-0.9775x - 0.2108y - 0.0113z + 6.2981 = 0$				16.9
3	C(1), C(2), C(3), C(8), C(9)	$-0.9815x - 0.1911y - 0.0150z + 6.2720 = 0$				38.3
4	C(1), C(3), C(8), C(9)	$-0.9803x - 0.1969y - 0.0148z + 6.2834 = 0$				0
5	C(2), C(8), C(9)	$-0.9823x - 0.1868y - 0.0151z + 6.2656 = 0$				0

Atom	Deviations of Atoms from Planes, Å				
	Plane 1	Plane 2	Plane 3	Plane 4	Plane 5
C(1)	-0.002 (2)	-0.024 (2) ^a	0.007 (2)	0.000 (2)	0.014 (2)
C(2)	-0.027 (3)	-0.053 (3)	-0.011 (3)	-0.022 (3)	0.000 (2)
C(3)	0.003 (2)	-0.017 (2) ^a	0.007 (2)	0.000 (2)	0.014 (2)
C(4)	0.003 (2)	0.003 (2)	-0.026 (2) ^a		
C(5)	-0.015 (2)	-0.005 (2)	-0.056 (2) ^a		
C(6)	-0.008 (2)	0.001 (2)	-0.046 (2) ^a		
C(7)	-0.008 (2)	0.004 (2)	-0.018 (2) ^a		
C(8)	0.005 (2)	-0.003 (2)	-0.001 (2)	0.000 (2)	0.000 (2)
C(9)	0.011 (2)	0.001 (2)	-0.001 (2)	0.000 (2)	0.000 (2)
N(1)	3.599 (2) ^a		3.587 (2) ^a		
N(2)	3.458 (2) ^a		3.478 (2) ^a		
Li	1.998 (3) ^a	1.979 (3) ^a	2.000 (3) ^a	1.996 (3)	2.007
H(1)					0.003 (17)
H(2)					0.026 (17)
H(3)					0.004 (17)

Dihedral Angles between Best Planes			
Plane 2-5	1.42°	Plane 2-4	0.84°
Plane 2-3	1.17°		

Best Weighted Least-Square Planes around the Li Atom					
Plane	Atoms in plane	Equation of plane			χ^2
6	C(2), C(8), Li, N(1), N(2)	$-0.1450x + 0.2552y - 0.9560z + 2.1092 = 0$			2031
7	C(2), C(8), N(1), N(2)	$-0.1452x + 0.2526y - 0.9566z + 2.1094 = 0$			70
8	C(2), C(8), Li	$-0.2068x + 0.2486y - 0.9463z + 2.4489 = 0$			0
9	N(1), N(2), Li	$-0.0592x + 0.2642y - 0.9626z + 1.9061 = 0$			0
10	C(2), Li, N(2)	$-0.1328x + 0.1572y - 0.9786z + 2.6067 = 0$			0
11	C(8), Li, N(1)	$-0.1699x + 0.3445y - 0.9233z + 1.9015 = 0$			0

	Deviations of Atoms from Planes					
	Plane					
	6	7	8	9	10	11
C(2)	0.001 (3)	-0.017 (3)	0	0.284 (3)	0	0.203 (3)
C(3)		-1.318 (3) ^a				
C(8)	0.017 (2)	0.006 (2)	0	0.322 (2)	0.245	0
Li	0.120 (3)	-0.132 (3) ^a	0	0	0	0
N(1)	0.003 (2)	-0.004 (2)	0.211 (2)	0	0.274	0
N(2)	0.021 (2)	0.006 (2)	0.245 (2)	0	0	0.299 (2)

Dihedral Angles			
6-5	83.7°	8-9	8.6°
7-5	83.7°	10-11	11.4°

^a Indicates atoms not included in the calculation of the best plane.

the cation, the more downfield the proton shift. Therefore, indenyllithium is a solvent separated species in DME or the LiTMEDA(sol)_x cation is larger than the Na(THF)_x cation. Using arguments which are consistent with previously reported nmr¹¹ results for carbonions, we conclude that indenyllithium TMEDA is a solvent separated ion pair in DME and about 75–95% solvent-separated in Et₂O and THF, respectively. The shifts in benzene may be due to solvent effects (see below) or the existence of indenyllithium TMEDA as a contact ion pair. If the latter is correct, the nmr of indenyllithium TMEDA in C₆D₆ and DME would then represent the two extremes of possible contact and solvent separated species. The approximation $\rho_{\text{nmr}} = \delta_{\text{benzene}}/k$, where δ_{benzene} is the proton resonance relative to benzene, $k = 10.7$, and ρ = electron density at the carbon atom directly associated with the proton, can be used to estimate the differences in the charge density in the p_z carbon orbitals of the contact and solvent separated species.¹² Con-

sidering various sources of error, the agreement between ρ_{INDO} and ρ_{nmr} (Table VIII) is good; *i.e.*, the agreement between calculated and observed changes in nmr chemical shifts is approximately 0.5 ppm for H(1) and better agreement is found for the other protons. The solid state geometry of indenyllithium TMEDA was used in the INDO calculations to represent the contact ion pair.

As noted above, another explanation for the shift to lower fields in benzene is the large magnetic anisotropy of the benzene molecule which can shift the anion proton resonances relative to the internal standard. Evidence for such an effect has been presented previously.¹³ Unfortunately, these compounds are not soluble enough in hexane to obtain good spectra, so that the magnitude of this effect cannot be evaluated. It remains as an alternative viable explanation for the downfield chemical shifts observed in the “nonpolar” solvent, benzene.

The upfield shift of the H(2) resonance (Figure 7) in

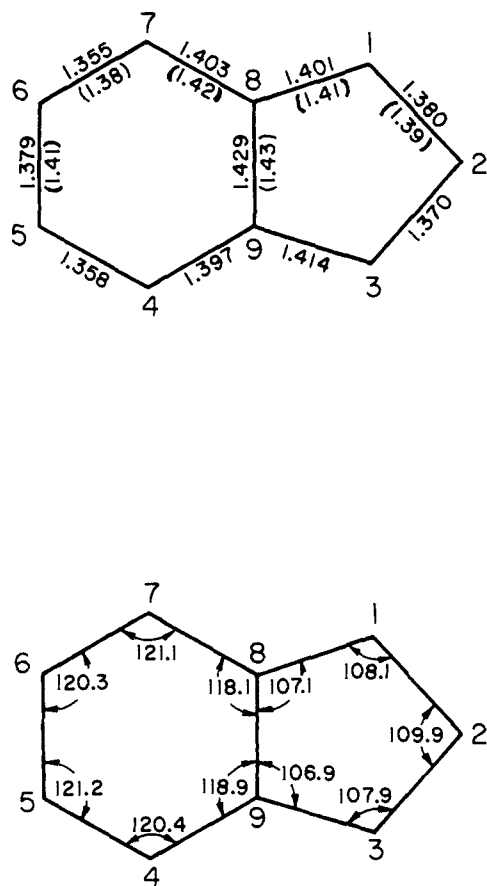


Figure 6. Molecular geometry of the indenyl group in $C_9H_7Li(N_2C_6H_{16})$. Distances given in parentheses are calculated from Hückel π bond orders.

Table VIII. Nmr Results for Indenyllithium

Cation	Solvent	Values for δ			
		H(1)	H(2)	H(4)	H(5)
Li	Benzene	6.35	6.81	7.78	6.97
Li	Et ₂ O	5.95	6.45	7.36	6.53
Li	THF	5.93	6.48	7.33	6.48
Li	DME	5.90	6.45	7.31	6.48
Na	THF	5.93	6.598	7.308	6.397

	Density in p_z Orbital					
	Benzene		DME		Solvent	
	ρ_{nmr}^a	ρ_{nmr}	ρ_{INDO}	ρ_{INDO}	Δ_{nmr}	Δ_{INDO}
C(1)	1.13	1.17	1.16	1.26	0.040	0.10
C(2)	1.065	1.099	1.02	1.05	0.034	0.03
C(4)	0.993	1.037	1.025	1.041	0.044	0.016
C(5)	1.042	1.088	1.05	1.095	0.046	0.045

^a $\rho_{nmr} = \rho_{benzene}/10.7$ corrected for ring currents in a neighboring ring by $\delta_1 = 12.0(a^2/R^3)$; T. Schaefer and W. G. Schneider, *Can. J. Chem.*, **41**, 966 (1963).

ether is indicative of a specific Li-C(2) interaction. This is particularly striking in that in indenylsodium (THF)^{11,12} the H(2)-H triplet is shifted downfield from the H(5), H(6) protons but is upfield to the H(5)-H, H(6)-H protons in indenyllithium (TMEDA). Therefore, the differences observed in the chemical shift of H(2) and H(5) for indenyl Li vs. indenyl Na can be attributed to differences in the metal indenyl interaction.

Summary

The studies of fluorenyllithium bisquinclidine,³ fluorenylpotassium tetramethylethylenediamine¹⁴ and indenylli-

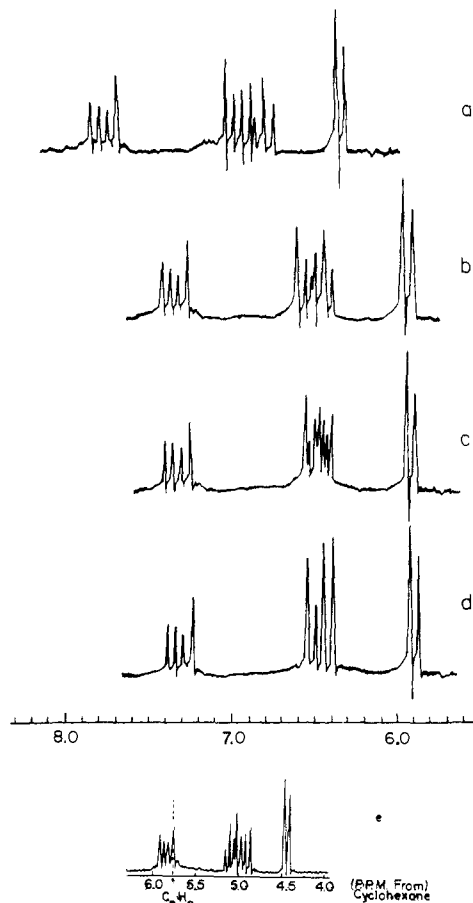


Figure 7. Nmr spectra of indenyllithium in (a) benzene, (b) ether, (c) tetrahydrofuran, and (d) dimethoxyethane at 60 MHz. The reference scale is in ppm relative to internal TMS. Cyclohexane proton resonance is -1.44 ppm relative to internal TMS. (e) Nmr spectrum of indenylsodium in THF (from ref 12).

thium tetramethylethylenediamine, along with the earlier studies of triphenylmethyl lithium tetramethylethylenediamine² and benzyl lithium triethylenediamine,¹ present a consistent picture of the bonding in these materials. The position of the disolvated lithium atom with respect to the delocalized carbanion is influenced not only by the maximization of ion dipolar interactions but also by the requirement that the lithium atom use all of its 2s and 2p orbitals in bonding if steric effects permit. In indenyllithium TMEDA, this is most effectively accomplished as discussed in the introductory section by a shift of the lithium atom from the allylic configuration observed in fluorenyllithium to a position above the five-membered ring. The effect of increased solvation remains to be studied; however, the approximate geometry for the potassium-fluorenyl pair is predicted by an electrostatic dipole model.

The geometries of the fluorenyl and indenyl carbanions, at least the difference in bond lengths, are predicted to a fair approximation by simple Hückel MO bond orders. The carbanions, however, are significantly nonplanar, with the most negatively charged carbon atom(s) displaced toward the lithium atom.

Acknowledgment. The support of the National Science Foundation under Grants NSFGH-33634 and NSFGP-31016X is gratefully acknowledged.

Supplementary Material Available. A listing of structure factor amplitudes will appear following these pages in the microfilm edition of this volume of the journal. Photocopies of the supplementary material from this paper only or microfiche (105 × 148 mm).

24X reduction, negatives) containing all of the supplementary material for the papers in this issue may be obtained from the Journals Department, American Chemical Society, 1155 16th St., N.W., Washington, D.C. 20036. Remit check or money order for \$5.00 for photocopy or \$2.00 for microfiche, referring to code number JACS-75-737.

References and Notes

- (1) S. P. Patterman, I. L. Karle, and G. D. Stucky, *J. Amer. Chem. Soc.*, **92**, 1150 (1970).
- (2) J. J. Brooks and G. D. Stucky, *J. Amer. Chem. Soc.*, **94**, 7333 (1972).
- (3) J. J. Brooks, W. Rhine and G. D. Stucky, *J. Amer. Chem. Soc.*, **94**, 7339 (1972).
- (4) J. J. Brooks, W. Rhine, and G. D. Stucky, *J. Amer. Chem. Soc.*, **94**, 7346 (1972).
- (5) D. Chang, R. V. Slaters, and M. Szwarc, *J. Phys. Chem.*, **70**, 3180 (1966).
- (6) R. E. Dessy, W. Kitching, T. Psorras, R. Salinger, A. Chen, and T. Chivers, *J. Amer. Chem. Soc.*, **88**, 460 (1966).
- (7) G. Germain, P. Main, and M. M. Woolfson, *Acta Crystallogr., Sect. B.*, **26**, 274 (1970).
- (8) See paragraph at end of paper regarding supplementary material.
- (9) J. L. Atwood and K. D. Smith, private communication, 1973. Comparisons of average bond lengths with true h^2 systems are probably somewhat risky, since in bis(indenyl)magnesium the h^2 distances vary from 2.31 to 2.54 Å for one indenyl group and 2.26 to 2.60 Å for a second.
- (10) See M. J. S. Dewar, "The Molecular Orbital Theory of Organic Chemistry," McGraw-Hill, New York, N.Y., 1969, p 166.
- (11) J. B. Grutzner, J. M. Lawlar, and L. M. Jackman, *J. Amer. Chem. Soc.*, **94**, 2306 (1972).
- (12) T. Schaefer and W. G. Schneider, *Can. J. Chem.*, **4**, 966 (1963).
- (13) R. Wasylstien, T. Schaefer, and R. Schwenk, *Can. J. Chem.*, **48**, 2085 (1970).
- (14) R. Zerger, W. Rhine, and G. Stucky, *J. Amer. Chem. Soc.*, **96**, 5441 (1974).
- (15) J. H. Burns and P. G. Laubereau, *Inorg. Chem.*, **10**, 2789 (1971).
- (16) N. C. Webb and R. E. Marsh, *Acta Cryst.*, **22**, 382 (1967).
- (17) L. Pauling, "The Nature of the Chemical Bond," Cornell University Press, Ithaca, N.Y., 1960, pp 385-392.

Computer Assisted Graph Theoretical Analysis of Complex Mechanistic Problems in Polycyclic Hydrocarbons. The Mechanism of Diamantane Formation from Various Pentacyclotetradecanes

Tamara M. Gund,^{1a} Paul v. R. Schleyer,* Peter H. Gund,^{1b} and W. Todd Wipke

Contribution from the Department of Chemistry, Princeton University, Princeton, New Jersey 08540. Received May 16, 1974

Abstract: The pentacyclotetradecane rearrangement graph culminating in diamantane (**1**) has been analyzed. The most probable mechanistic pathways from tetrahydro-Binor-S (**2** or **3**), hydrogenated Katz [2 + 4] norbornadiene dimers (**7** and **8**), and [2 + 2] norbornene dimers (**9**, **10**, and **11**) were deduced by graphical analysis guided by empirical force field (strain) calculations. Graphs of isomeric hydrocarbons were generated from a chosen precursor by 1,2-alkyl shifts, employing the simulation and evaluation of chemical synthesis (SECS) computer program. Due to the extremely large number of possible intermediates, it was necessary to simplify graph generation by adopting certain assumptions. From a given hydrocarbon precursor, all possible 1,2-shift isomers were generated and their strain energies calculated. The resulting isomer with lowest energy was processed further. Graph generation proceeded in this manner until diamantane was reached. The most probable mechanism for isomerization of **2** or **3** → **1** is proposed to involve, in sequence, *trans*-pentacyclo-[8.2.1.1^{2,5}.0^{3,7}.0^{8,12}]tetradecane (**6**), a tetrasubstituted intermediate (**24**), **28**, and protodiamantane (**29**). In the actual reaction, **6** was found to be the last isolable intermediate, as predicted by the strain energy calculations. When structures with tetrasubstituted cations were excluded from the graph, sets of interconverting pentacyclotetradecane isomers were obtained. The sets considered were derived from the [2 + 2] norbornene dimer **11** (6 structures), from the [2 + 4] hydrogenated Katz norbornadiene dimer **7** (10 structures), from tetrahydro-Binor-S (**2**) (13 structures), from **28** (293 structures, designated family [1,2,4] [3,5,6]), and from diamantane (**1**) (119 structures, family [1,3,5] [2,4,6]). Experimentally, isomerization to the lowest energy isomer within each family prior to further reaction *via* tetrasubstituted intermediates appears to take place, and the yield of diamantane decreases with the number of family boundaries which must be crossed.

Lewis acid catalyzed isomerizations of hydrocarbons are complex, thermodynamically controlled carbocation processes.² Skeletal transformations, *e.g.*, that giving adamantane,^{2b} involve hydride abstractions and multiple Wagner-Meerwein rearrangements. Since the number of possible intermediates and reaction pathways may be astronomically large, the determination of the detailed mechanism can be exceedingly difficult.

Such complex systems require systematic analysis. The first pertinent approach appears to be that of Balaban, Farcasiu, and Banica,³ who developed a graphical treatment interrelating all structures interconvertible by 1,2 shifts, which allowed calculation of the number of possible isomers and pathways. For hypothetically labeled ethyl cations, automerization, *e.g.*, $H_1H_2H_3C_1^+ \rightleftharpoons C_2H_4H_5 \rightleftharpoons H_4H_5C_1^+ \rightleftharpoons C_2H_3H_2H_1$, etc., involves 20 possible classical cations interconvertible by 30 1,2 shifts. The propyl cations are similarly

interconverted with a possible intermediacy of 1680 isomers and 3150 pathways. Application of this approach to larger, nondegenerate systems is, however, extensively complex unless assumptions reducing the number of isomers and pathways are made.

Whitlock and Siefken⁴ analyzed the possible mechanisms for adamantane formation from *endo*-tetrahydrodicyclopentadiene and other tricyclodecane by means of a similar graphical method. A graph was generated by assuming all possible 1,2-alkyl shifts. Simplification was achieved (1) by considering only hydrocarbons and omitting cations from the graph, (2) by excluding all highly strained structures, *e.g.*, those containing three- and four-membered rings, and (3) by excluding structures formed from primary cation intermediates, *e.g.*, alkyl substituted isomers. A chemical graph containing 16 C₁₀H₁₆ tricyclodecane isomers resulted. By actual count, 2897 different pathways for inter-